


# Mesoscale oceanographic meanders influence protist community function and structure in the southern Indian Ocean

Daniela Sturm<sup>1,2</sup>  | Joost de Vries<sup>3</sup> | William M. Balch<sup>4</sup> | Glen Wheeler<sup>1</sup> | Colin Brownlee<sup>1</sup>

<sup>1</sup>The Marine Biological Association, Plymouth, UK

<sup>2</sup>School of Ocean and Earth Science, University of Southampton, Southampton, UK

<sup>3</sup>BRIDGE, School of Geographical Sciences, University of Bristol, Bristol, UK

<sup>4</sup>Bigelow Laboratory for Ocean Sciences, East Boothbay, Maine, USA

## Correspondence

Glen Wheeler and Colin Brownlee, The Marine Biological Association, The Laboratory, Citadel Hill, Plymouth, Devon PL1 2PB, UK.

Email: [glw@mba.ac.uk](mailto:glw@mba.ac.uk) and [cbr@mba.ac.uk](mailto:cbr@mba.ac.uk)

## Funding information

H2020 European Research Council, Grant/Award Number: ERC-ADG-670390; Leverhulme Trust, Grant/Award Number: EM-2021-067; National Science Foundation (NSF), Grant/Award Number: OCE-1735664; Natural Environment Research Council, Grant/Award Number: NE/SO07210/1

## Abstract

The interface between the nutrient-rich Southern Ocean and oligotrophic Indian Ocean creates unique environmental conditions that can strongly influence biological processes. We investigated protist communities across a mesoscale meander of the Subtropical Front within the Southern Indian Ocean. 18S V9 rDNA metabarcoding suggests a diverse protist community in which the dinoflagellates and parasitic Syndiniales were abundant. Diversity was highest in frontal waters of the mesoscale meander, with differences in community structure inside and outside the meander. While the overall community was dominated by mixotrophic taxa, the frontal boundary of the meander had increased abundances of heterotrophic taxa, with potential implications for net atmospheric CO<sub>2</sub> drawdown. Pulse amplitude modulated (PAM) fluorimetry revealed significant differences in the photo-physiology of phytoplankton communities inside and outside the meander. By using single-cell PAM microscopy, we identified physiological differences between dinoflagellate and coccolithophore taxa, which may have contributed to changes in photophysiology observed at community level. Overall, our results demonstrate that frontal areas have a strong impact on the composition of protist communities in the Southern Ocean with important implications for understanding biological processes in this region.

## INTRODUCTION

Mesoscale oceanographic features spanning tens to hundreds of kilometres are recognized to be one of the main drivers controlling spatio-temporal variations of biological production (Glover et al., 2018; Hernández-Hernández et al., 2020). Eddies or meanders (noncircular propagations of currents, collectively defined as coherent mesoscale structures) often originate from large-scale currents or fronts and supply nutrients into the euphotic zone allowing phytoplankton to thrive in otherwise nutrient-poor regions (Pingree et al., 1975, 1979). Previous research identified higher primary production within a mesoscale eddy in the Mediterranean,

accompanied by high abundances of phytoplankton and increased abundance of zooplankton and heterotrophic bacteria (Belkin et al., 2022). Frontal regions therefore likely play an important role in determining the diversity of marine microbial communities. Molecular methods that allow high resolution analysis of community structure, are increasingly used to study marine microbes (De Vargas et al., 2015). Analysis of protist communities in the western North Atlantic using 18S rDNA sequencing revealed greatest diversity within the Gulf Stream, one of the world's largest mesoscale systems (Countway et al., 2007). Differences were also observed between protist communities inside and outside an area impacted by the passage of mesoscale

This is an open access article under the terms of the [Creative Commons Attribution](https://creativecommons.org/licenses/by/4.0/) License, which permits use, distribution and reproduction in any medium, provided the original work is properly cited.

© 2023 The Authors. *Environmental Microbiology* published by Applied Microbiology International and John Wiley & Sons Ltd.

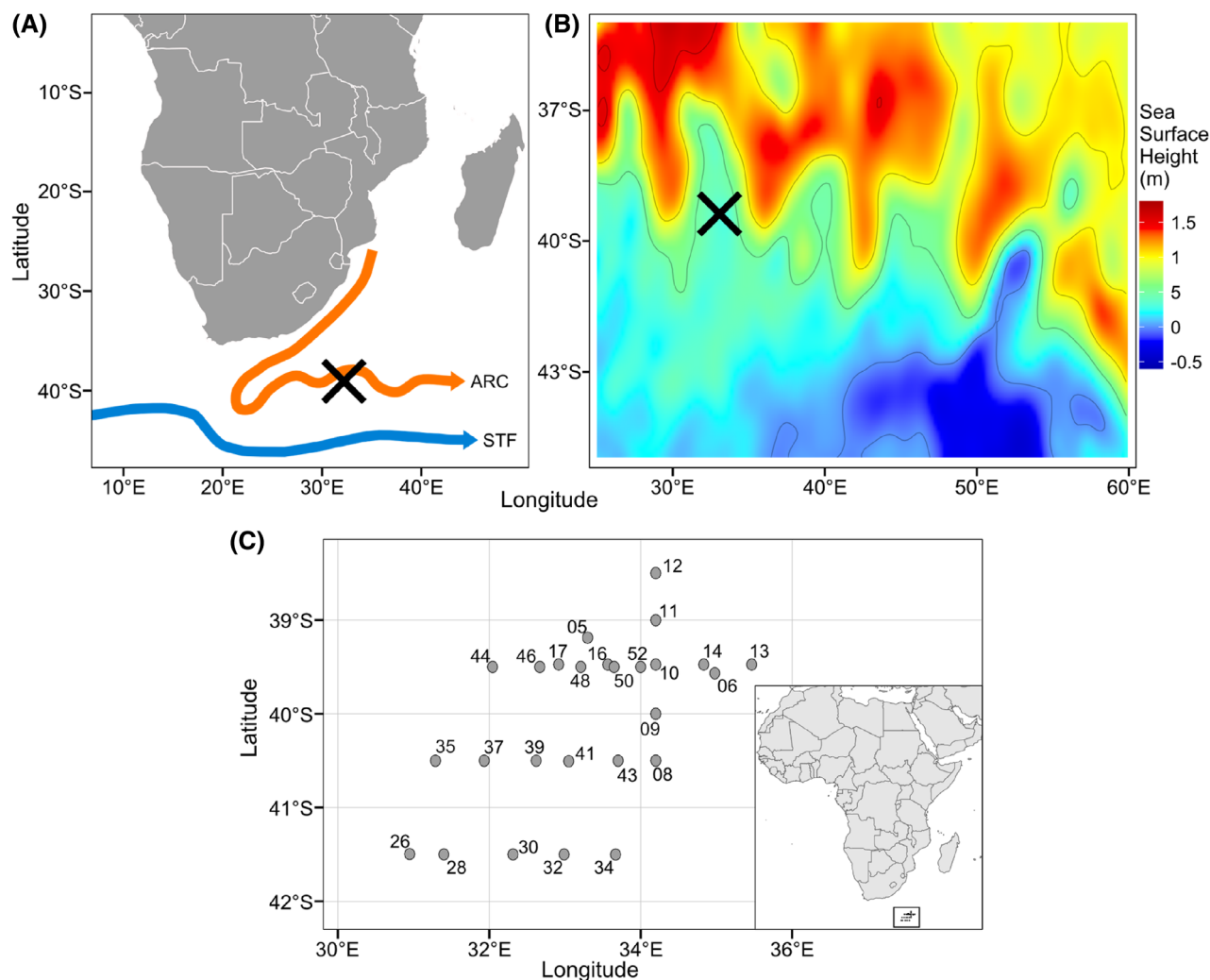


**FIGURE 1** Frontal regions and inherent mesoscale meanders in the Southern Indian Ocean region and study area. (A) Major frontal systems in the Southern Indian Ocean are the Agulhas Return Current frontal region (orange, ARC) and the Southern Subtropical Front (blue, STF). Black cross: area of interest. (B) Absolute Dynamic Topography along the STF showing mesoscale meanders. Black cross: area of interest. (C) Map of the sampling region in the Southern Indian Ocean (inlet) and microbial sampling stations for metabarcoding and fluorimetry analysis.

eddies in the Sargasso Sea (Blanco-Bercial et al., 2022).

Mesoscale features are prevalent in the Southern Ocean (SO), an important region for primary production and carbon cycling, with uptake of over 40% of anthropogenically produced  $\text{CO}_2$  occurring south of  $30^\circ\text{S}$  (Frölicher et al., 2015; Landschützer et al., 2015). Circulation in the SO is dominated by the Antarctic Circumpolar Current and two associated oceanographic fronts: the Subtropical convergence (Subtropical Front [STF]), which separates subtropical from subpolar waters, and the Antarctic convergence separating Sub-Antarctic and Antarctic waters (Gordon, 1967). The Indian sector of the SO (SIO) is more complex than the Atlantic and Pacific sectors due to the presence of an additional frontal boundary, the Agulhas Return Current (ARC), just north of the STF

around  $40^\circ\text{S}$  (Lutjeharms and El Lutjeharms & Valentine, 1984; Figure 1A). The SIO is generally depleted in nutrients crucial for phytoplankton growth such as iron (Fe) and silicate (Si) (Longhurst, 1998). However, mesoscale oceanographic features can impact biological productivity in this region. Patches of high chlorophyll associated with a quasi-isolated nutrient-rich ARC ring exhibited sustained biological production over large spatial and temporal time scales in an otherwise nutrient-depleted gyre (Lehahn et al., 2011).

The SO is predicted to be uniquely impacted by climate change, which, due to the important role of this region in the carbon cycle, might thus substantially influence the global climate. Complex changes in eddy-mediated transport have been caused by an increase in Antarctic winds over the past 30 years strengthening

wind-induced Ekman transport which will lead to increased nutrient upwelling (Arrigo et al., 2008; Li et al., 2021). Since the 1980s, an increase in wind stress has further led to a significant warming trend in the Agulhas current system (Rouault et al., 2009). Satellite and hydrographic data further show a corresponding southward shift of the STF (Alory et al., 2007).

To understand how mesoscale oceanographic features and their potential future changes will impact biological processes, we need to know how these features influence microbial communities. Marine microbial communities comprise prokaryotes and eukaryotes, with the latter primarily represented by single-celled protists of diverse taxa with wide ecological roles. They include photo- and mixotrophic species, as well as heterotrophs (Caron et al., 2009; Mitra et al., 2016). Trophic strategy influences the fate of carbon in terrestrial and marine systems. CO<sub>2</sub> is released by systems where heterotrophy is the dominant trophic strategy, while net phototrophic systems sequester CO<sub>2</sub>. Protist community composition also influences other important biogeochemical processes, such as nutrient uptake and recycling, and carbon sequestration to the deep ocean via sinking (Rembauville et al., 2017; Weber & Deutsch, 2010). Most surveys of marine protist diversity have focused on tropical and temperate regions in the northern hemisphere, with the SO remaining relatively understudied. Within the Indian sector of the SO, studies have focussed almost exclusively on the Crozet and Kerguelen Islands where natural iron supply from iron-rich deep waters relieves the general iron limitation of the SO (Christaki et al., 2015; Christaki et al., 2021; Georges et al., 2014; Sassenhagen et al., 2020). There is a need to better understand the microbial communities in the wider SO in order to establish the influence of mesoscale oceanographic features on biological processes in this region.

In addition to changes in community composition, microbes within mesoscale features may undergo spatial or temporal changes in physiology that contribute to the overall productivity of the community. The photosynthetic performance of phytoplankton communities is commonly studied using chlorophyll fluorimetry (Suggett et al., 2003, 2009). Photosynthetic efficiency (Fv/Fm) has often been used as an indicator of phytoplankton 'health', with lower values often associated with sub-optimal photosynthetic performance due to environmental stress caused by nutrient limitation or excess light (Kromkamp & Forster, 2003; Moore et al., 2003). However, the interpretation of these datasets in natural communities is complex, as the parameters may be influenced by changes in community composition as well as physiological status (Suggett et al., 2009). One potential way to address this issue is through the development of imaging approaches to measure photosynthetic parameters in individual phytoplankton cells (Oxborough, 2004). Pulse amplitude

modulated (PAM) imaging has been used previously to specifically assess changes in the photophysiology of diatom cells within a mixed community in an Antarctic mesocosm experiment (Petrou et al., 2019), although to our knowledge has not yet been applied to the study of natural phytoplankton populations in situ.

In this study, we have used high-throughput sequencing with metabarcoding to identify the protist assemblage of a mesoscale meander of the STF in the Southern Indian Ocean during austral summer. We aimed to determine which protist groups dominate the surveyed area and, whether community structure and diversity differed across the meander. We also examined photophysiology using chlorophyll fluorimetry at the community and single-cell levels to evaluate whether significant functional differences occurred across the meander. Our results indicate a complex interplay between relative protist abundance and group-specific physiological properties that determine the overall functional properties of the protist community.

## EXPERIMENTAL PROCEDURES

### Study area and sampling

Samples for this study were taken onboard the R/V Thomas G. Thompson (TN376) in the Southern Indian Ocean (Figure 1C) between 30 January and 21 February 2020 (38.5–41.5 °S, 30.9–35.5 °E). We sampled 26 locations within a mesoscale meander system measuring over 80,000 km<sup>2</sup> (400 km long and 200 km wide) which had pinched off northward from the Southern STF and embedded within a meander of the ARC. In the north-eastern section of the meander, conductivity temperature depth (CTD) instrument samples were taken as a cross section and included warmer and saltier areas at the boundary and the periphery of the meander. In the centre, zonal transects were carried out from west-to-east.

### Sample collection CTD

Samples for metabarcoding and fluorimetry analysis were collected at each station from the surface (SA; sampled from the uppermost Niskin bottle at depths between 2 and 12 m) and from the deep-chlorophyll maximum (DCM; determined by CTD downcast as maximum chlorophyll fluorescence at depths between 9 and 60 m) in Niskin bottles mounted on a CTD-rosette. Approximately 1 litre of water was collected in acid-cleaned bottles (1.5% HCl), which were rinsed with Milli-Q water and subsequently with sampling seawater at the respective station. Samples were filtered through 0.45 µm pore size, 47 mm diameter membrane

filters (Supor<sup>®</sup>, Pall, UK) using vacuum filtration. The exact amount of filtration was dependent on local biomass and fluctuated between 500 and 1000 mL to avoid clogging of the filters. No pre-filtration was carried out, as the abundance of metazoans was negligible. Samples were preserved in RNAlater (Invitrogen, USA) to preserve nucleic acids and stored at  $-80^{\circ}\text{C}$ .

Samples for scanning electron microscopy (SEM) were taken and analysed as described in Sturm et al., 2022.

## Hydrographic conditions and nutrients

Temperature, salinity, and chlorophyll a fluorescence were measured using a Seabird SBE 9 CTD (Sea-Bird Scientific, USA), mounted on the rosette containing 24 Niskin bottles.

Dissolved inorganic nutrients (nitrate, nitrite, ammonium, phosphate, silicate) and dissolved oxygen analysed were carried out onboard by the Scripps Oceanographic Data Facility (ODF) group according to the methods used by Atlas et al., 1971; Hager et al., 1972; and Gordon et al., 1993. For detailed methods see Scripps Chemistry Services <https://scripps.ucsd.edu/ships/shipboard-technical-support/odf/chemistry-services>. Values for nitrate, nitrite, and ammonium were combined for total dissolved inorganic nitrogen (DIN).

## DNA extraction, amplification, and sequencing of rDNA fragments

Filters for DNA analysis were processed with the Zymo-BIOMICS DNA Miniprep Kit (Zymo Research, USA) according to manufacturer's instructions. Purity and quality of the extracted DNA were assessed with Nanodrop. Library preparation and sequencing were conducted by the NU-OMICS facility at Northumbria University, UK (<https://earthmicrobiome.org/protocols-and-standards/18s/>). Samples were amplified by polymerase chain reaction (PCR) using the universal eukaryotic primers Illumina\_Euk\_1391f and Illumina\_EukBr (Amaral-Zettler et al., 2009) targeting the hypervariable V9 region of the nuclear gene that encodes 18S rRNA (Table S1). The V9 18S region was chosen for this study as it is used by other large-scale metabarcoding studies such as the TARA Oceans expedition, allowing us to put our data into a global context (De Vargas et al., 2015). The V9 region was further found to demonstrate improved accuracy of eukaryotic phytoplankton community composition (Bradley et al., 2016), as well as being less prone to generating PCR biases and allowing the discrimination of taxa over a greater phylogenetic depth compared with other

commonly used marker regions such as V4 (Catlett et al., 2020; De Vargas et al., 2015).

Sequencing was conducted on an Illumina MiSeq using 250 + 250 bp paired-end V3 chemistry. Sequence and metadata are accessible through the NCBI Sequence Read Archive (SRA) under accession number PRJNA952565.

## Sequence processing

Raw reads were pre-processed using 'Cutadapt' to remove adapter sequences, primers, and other types of unwanted sequences (Martin, 2011). We processed paired-end reads according to the 'DADA2' pipeline (Callahan et al., 2016) in R-3.5.1. Reads were truncated and trimmed to remove low quality reads and primers, respectively. At most 2 (forward reads) and 3 (reverse reads) errors were allowed during filtering. Settings of 'filterAndTrim' were set to `truncLen=c(130,120), maxN=0, maxEE=c(2,3), truncQ=2, rm.phix=TRUE`. After dereplicating forward and reverse reads, amplicon sequence variants (ASVs) were resolved at single nucleotide resolution. Compared with traditional operational taxonomic units (OTUs), this method provides greater accuracy and reproducibility (Callahan et al., 2016). Subsequently, paired-end reads were merged, and chimeras identified and removed using the 'removeBimeraDevono' function of DADA2 in R. Approximately 3% of merged reads were identified as chimeric. The taxonomy of ASVs was assigned in DADA2 using 'assignTaxonomy' with the naive Bayesian classifier method and the PR<sup>2</sup> database from Guillou et al. (2012) modified by De Vargas et al., 2015 to refine taxonomic assignments to the V9 18S region (V9\_PR<sup>2</sup> database W2 from De Vargas et al., 2015). Read numbers per sample ranged from 34,167 to 176,819 with a mean of 56,877 reads. Sequence reads were randomly subsampled to an even depth of 34,167 reads per sample. ASVs classified as Archaea, Bacteria, Metazoa, Streptophyta, and Fungi were removed from the dataset before subsequent analysis of protist community. Roughly 14% were unassigned at taxonomic ranks 'below' Kingdom, that is, were classified as unknown Eukaryotes (~28% at Phylum level). As many of these ASVs may represent clades for which no corresponding sequence is available, they were not removed from the dataset. Data were transformed to relative abundances using the 'transform:compositional' function within the 'microbiome' package. For ordination and IndVal analyses, rare ASVs were pruned prior to transformation to avoid skewing of major trends. ASVs were considered as rare when they occurred less than three times in < 10% of samples.

## Protist biogeography

Statistical analysis was carried out in R and metabarcoding data were explored using R package ‘phyloseq’ (McMurdie & Holmes, 2013) and figures were made with ‘ggplot2’ (Wickham et al., 2016). To compare the protist community within and outside the meander, we divided the sampled stations into ‘centre’, ‘boundary’, and ‘outside’ regions based on salinity and temperature characteristics of each station. Initial salinity (and temperature) ranges were defined as 34.5–34.9 and 35.1–35.6 PSU (and 14.2–16.1 and 16.4–21.2°C) for ‘centre’ and ‘outside’, respectively. Values that were intermediate or only within these categories for one parameter were classified as ‘boundary’. The assignments were then checked against location data, and adjusted where appropriate.

We compared alpha community diversity indices between the meander regions using a non-parametric Wilcoxon rank-sum test. Alpha community metrics include Shannon diversity ( $H'$ ), ASV richness, and ASV Evenness and were calculated using the ‘estimate\_richness’ function within the ‘phyloseq’ package.

Assemblage-wide variation in protist response within the surveyed area were determined via ordination by non-metric multidimensional scaling (NMDS) based on Bray–Curtis dissimilarity coefficients. Vectors for environmental variables were plotted using the function ‘envfit’. To determine whether the centroids of the NMDS clusters are significantly different, we computed permutational multivariate analysis of variance (PERMANOVA) based on the Bray–Curtis distance matrix (Anderson, 2001). We used analysis of similarity (ANOSIM) between the three factors to confirm that distances between groups are greater than within groups. To confirm that the use of relative ASV abundances did not influence these analyses, we re-analysed certain datasets using a centred log ratio transformation and found no substantial differences from our initial analysis.

To identify which clades contribute most to the response of the protist assemblage to the meander locations, we used indicator value analysis (IndVal, Dufrene & Legendre, 1997). IndVal assesses the degree of fidelity (frequency of occurrence) and specificity (mean abundance within a cluster compared with the other clusters) of an ASV to a given factor and is therefore superior to analysis of mere abundance.

To determine shifts in trophic mode across the meander locations, we selected a sub-set of the 24 most abundant phyla based on their associated ASV abundances, and categorized these phyla into their respective primary or predominant trophic strategies based on information available in the ‘World Register for Marine Species’ (WoRMS) and literature review of specific taxa (Table S2). We then summarized the relative abundances of phyla to obtain the

proportion of each trophic strategy at all stations and their inherent meander locations.

## Analysis of photosynthetic parameters in situ and in cultures

To obtain community values of the photosynthetic parameters  $F_v/F_m$  (maximum quantum yield of photosystem II), NPQ (non-photochemical quenching), and ETR (electron transport rate; for full definitions see Table S3), triplicate seawater samples were taken from the Niskin bottles and dark-adapted at in situ temperature for >30 min prior to analysis. Experimental measurements were made with a PAM fluorimeter (Water-PAM, Walz, Germany) with 3 mL cuvette samples.

PAM analysis of single-cell chlorophyll fluorescence was carried out with a modified PAM microscope (Photon Systems International [PSI], Cz), allowing images of  $F_o$ ,  $F_m$ , and  $F_v$  by using LED arrays to provide measuring pulses and actinic light (Figure 7C). Measurements were restricted to  $F_v/F_m$  and calm conditions since slow focus drift associated with vertical movements of the ship prevented reliable measurement of NPQ, quantum efficiency (QII), and ETR. The microscope also allowed acquisition of bright field and polarized light images to identify individual phytoplankton cells and calcifying coccolithophores. Cells were allowed to settle in darkness for >1 h before transfer to the microscope imaging chamber, which comprised a glass-bottomed dish and  $\times 20$  or  $\times 40$  Zeiss water immersion objectives (numerical aperture 0.5 and 1.0, respectively). The dish was mounted on a temperature-controlled perfusion cell, which allowed cells to be maintained at the precise collection temperature. All manipulations were carried out in darkness. Bright field images were obtained using far red light, which does not activate the PSII reaction centres. Images were analysed using PSI FluorCam7 software. For acquisition and analysis of photosynthetic parameters of representative cultured taxa, we chose several strains of dinoflagellates, diatoms, and haptophytes from the Plymouth and Roscoff Culture Collection (Table S4). Cultures were grown in sterile-filtered F/2 seawater media (Guillard, 1975) under a cycle of 14 h:10 h light:dark ( $80 \mu\text{mol photons m}^{-2} \text{s}^{-1}$ ) at 15°C. Growth was monitored regularly with cell counts and photosynthetic parameters were acquired during mid-exponential growth.

## Correlation analysis and interpolation maps

Diversity indices, species abundances, and photosynthetic parameters were tested for correlations with

environmental parameters using Spearman's Rank correlations using function 'cor.test' from the 'stats' R package. Correlation results were reported if squared correlation coefficient ( $R^2$ ) > 0.1, and  $p < 0.05$ . To visualize physical and biological parameters, we interpolated values using the multilevel B-spline approximation (MBA) algorithm described by Lee et al., 1997 with the 'mba.surf' function from the 'MBA' R package.

## RESULTS

### Distinct physical and chemical properties of the meander

We sampled a mesoscale meander feature within the Southern Indian Ocean derived from the Southern Subtropical Front. Satellite imagery (MODIS-Aqua) indicated high chlorophyll and high particulate inorganic carbon (PIC; implying coccolithophore abundance) in this feature. Profiles of sea surface height illustrate that these meander systems extend thousands of km further east, suggesting that the findings of this study may be applicable over a much larger area (Figure 1B).

Measurements of temperature and salinity were used to categorize the sampling stations into three regions (centre, boundary or outside). The centre of the meander was significantly cooler and fresher than its periphery, which was characterized by the higher temperature and salinity waters originating from the Agulhas front (Figure 2A,B). The meander was further characterized by significantly higher nutrients (DIN and phosphate), dissolved oxygen, and chlorophyll fluorescence. The boundary between the centre and outside of the meander formed an intermediate environment with respect to these parameters.

### Dinoflagellates are prominent within the Southern Ocean protist community

18S rDNA metabarcoding identified a total of 4013 ASV for the 51 sampling points. The largest proportion of ASVs belonged to members of the Alveolata, with a total of 2474 assigned ASVs (Figure 3A). The majority of ASVs within this group were affiliated to the predominantly mixotrophic flagellated Dinophyceae, the parasitic Syndiniales and the ciliated Spirotrichea, with these three groups representing the most abundant phyla within the overall community (48.8%, 21.7%, and 3.1%, respectively; Figure 3B and Table S5). Within the Dinophyceae, the most abundant ASVs are assigned to *Lepidodinium viride*, *Enciculifera imariensis*, *Prorocentrum micans*, *Pentaparsodinium* sp., and *Azadinium galwayense*.

Other groups exhibiting a lower relative abundance include the photosynthetic Prymnesiophyceae (2.7%), the heterotrophic marine stramenopiles MAST (2.1%), the photosynthetic stramenopiles Bacillariophyta (diatoms, 1.9%), and the green algae group Prasino-Clade-7 (1.6%). Also present were the phototrophic Pelagophyceae (1.5%), the green algae Mamiellophyceae (1.3%) and the flagellated alveolates Discoba (0.7%).

The distribution of these higher taxonomic ranks was relatively similar across all sampling stations, with the exception of Station 11\_SA (outside meander), which exhibited a much higher abundance of Bacillariophyta (24.4%). 93% of the Bacillariophyta ASVs at this station were assigned to the diatom *Pseudo-nitzschia pungens*.

### Differences in community composition across the meander

IndVal analysis was used to assess which phyla were indicative of each of the three regions. Multiple rhizarian groups (Acantharea, Polycystinea, and RAD-C) were enriched at the meander boundary, along with the alveolates Syndiniales and the excavates Euglenozoa (Table 1). Groups primarily associated with the meander centre included the groups Pyramimonadales and Prasino-Clade-9 (both Archeplastida), as well as Discoba (Excavata), and the Dinophyceae (Alveolata). Multiple stramenopile groups were identified as indicators of the region outside of the meander, including the Dictyochophyceae, MAST, Chrysophyceae-Synurophyceae, Pelagophyceae, and Bolidophyceae. Additionally, the Katablepharidaceae of the Hacrobia supergroup and the Spirotrichea of the Alveolata were classified by IndVal as predictors of the region outside the meander. IndVal analysis at the ASV level identified specific ASVs, primarily belonging to the dinoflagellate and marine alveolate (MALV I, MALV II) clades, that were associated with each region (Table S6).

Using the dominant trophic modes for each of the groups, we assessed whether the different regions exhibited differences in overall trophic strategy. The community was comprised of  $50.5\% \pm 8.5\%$  mixotrophic phyla,  $29.7\% \pm 5.7\%$  heterotrophic phyla, and  $10.1\% \pm 5.7\%$  phototrophic phyla, with  $9.7 \pm 2.4\%$  phyla of unknown trophic level. Most stations were dominated by mixotrophic phyla, although stations 9\_SA and 30\_DCM were mainly comprised of heterotrophs, while station 11\_SA was dominated by phototrophs (Figure 4A).

Mixotrophs were dominant throughout the centre, boundary, and outside of the meander. However, heterotrophs exhibited an increased abundance at the meander boundary (Figure 4B), with specific groups of grazing heterotrophs significantly more abundant outside the meander. These include the Spirotrichea

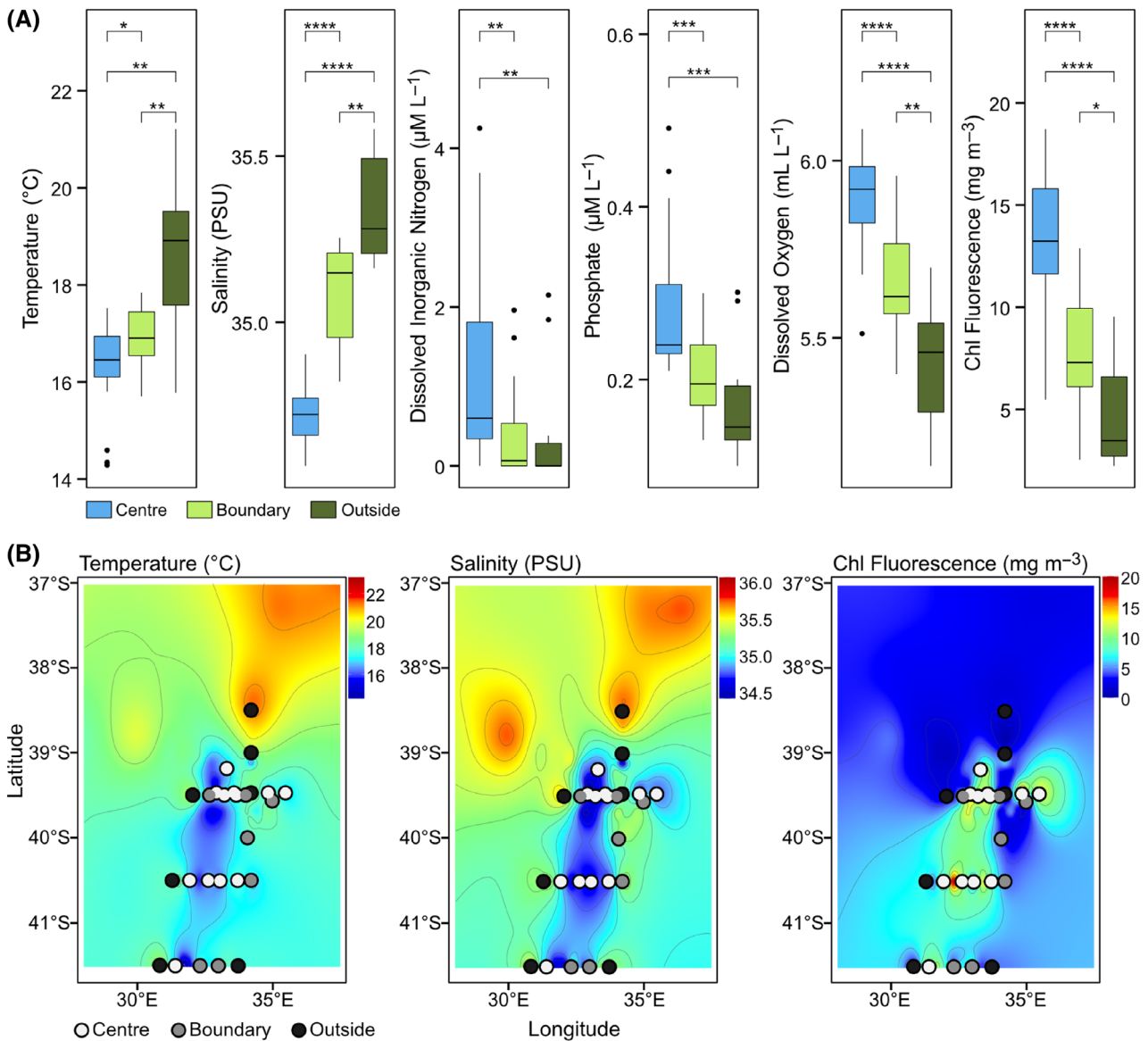


**FIGURE 2** Environmental conditions across the Subtropical Front mesoscale meander (A) Temperature, salinity, dissolved inorganic nitrogen, phosphate, dissolved oxygen, and chlorophyll fluorescence at centre (blue), boundary (light green), and outside (dark green) of the meander. Boxplot centre lines represent median, box hinges indicate Quartiles 1 and 3, and whiskers 1.5 Interquartile Range from hinge or furthest data point, whichever is closer. Black dots indicate outliers. Means between groups were compared using Wilcoxon rank-sum test: \*\*\*\* $p < 0.0001$ , \*\*\* $p < 0.001$ , \*\* $p < 0.01$ , \* $p < 0.05$ . (B) Temperature, salinity, and chlorophyll fluorescence highlight the meander characteristics. CTD stations defined as the centre (white), boundary (grey), and outside (black) of the meander are overlaid.

( $p < 0.05$ ), the Katablepharidaceae ( $p < 0.01$ ), and the MAST group ( $p < 0.001$ ). The relative abundance of phototrophs did not change significantly, but was more variable outside of the meander where it ranged from 6% to 38%.

### Highest protist diversity at the meander boundary

Analysis of community diversity within stations showed significantly higher ASV evenness, richness, and

Shannon index at the boundary of the meander compared with its centre (Figure 5A). Additionally, richness and Shannon index were significantly greater at the boundary of the meander compared with its outside. NMDS ordination based on Bray–Curtis dissimilarity shows a clear transition in protist community composition between the centre of the meander, to its boundary, and outside (Figure 5B). Multiple regression analysis of environmental variables using envfit (NMDS vector overlay) determined that temperature is the only significant predictor of community structure ( $p < 0.05$ ). ANOSIM confirmed that the differences between groups are larger

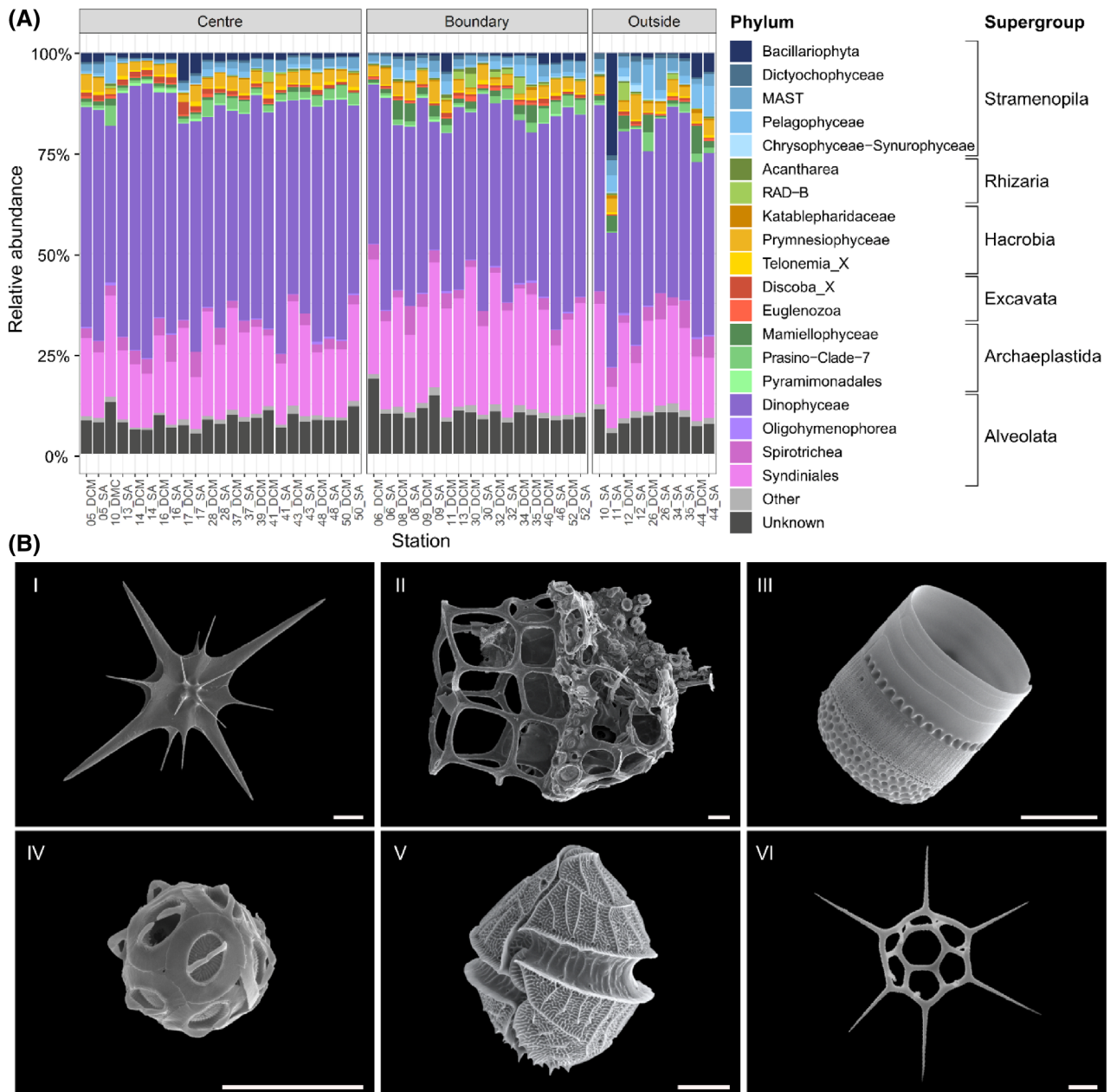


**FIGURE 3** Protist composition across the Indian sector of the Southern Ocean mesoscale meander. (A) Relative protist community composition of top 20 phyla at all stations grouped by the centre, the boundary, and the outside of the meander. (B) Representative scanning electron microscopy images from the most abundant protist groups in the surveyed area. (I) radiolarian Clade E/F (Acantharea), (II) tintinnid *Dictyocysta* sp. (Spirotrichaea), (III) diatom *Thalassiosira* sp. (Bacillariophyta), (IV) coccolithophore *Gephyrocapsa oceanica* (Prymnesiophyceae), (V) dinoflagellate *Gonyaulax striata* sensu Dodge 1989 (Dinophyceae), (VI) silicoflagellate *Dictyocha speculum* (Dictyophyceae). Scale bar 5  $\mu\text{m}$ .

than within groups ( $p < 0.001$ ,  $R = 0.44$ ), and PerMANOVA further showed that the centroids of each cluster are significantly different ( $p.\text{adj} < 0.01$ ). A Venn diagram of shared ASVs across meander locations illustrates highest overlap between the boundary and centre environment (533 shared ASVs) and lowest overlap between the outside and centre of the meander (70 shared ASVs), while 1180 ASVs were shared across all regions of the meander (Figure 5C).

All three diversity indices were negatively correlated with latitude, however, ASV evenness only showed a very weak correlation (Shannon  $R^2 = 0.15$ ,  $p < 0.01$ ; ASV richness  $R^2 = 0.17$ ,  $p < 0.01$ , ASV evenness  $R^2 = 0.08$ ,  $p < 0.05$ ). ASV evenness and the Shannon Index were additionally positively correlated with salinity ( $R^2 = 0.14$ ,  $p < 0.01$  and  $R^2 = 0.12$ ,  $p < 0.05$ , respectively), but no other parameter had a significant relationship with these alpha-diversity measures.



TABLE 1 Classification of protist indicator phyla by IndVal analysis across the different meander locations.

Phylum	Supergroup	IndVal classification	IndVal stat	IndVal <i>p</i>
Syndiniales	Alveolata	Boundary	0.603	0.001***
Acantharea	Rhizaria	Boundary	0.515	0.001***
Euglenozoa	Excavata	Boundary	0.423	0.009**
Polycystinea	Rhizaria	Boundary	0.380	0.032*
RAD-C	Rhizaria	Boundary	0.367	0.020*
Dinophyceae	Alveolata	Centre	0.596	0.001***
Discoba_X	Excavata	Centre	0.552	0.001***
Pyramimonadales	Archaeplastida	Centre	0.425	0.010**
Prasino-Clade-9	Archaeplastida	Centre	0.345	0.046*
Dictyochophyceae	Stramenopiles	Outside	0.567	0.002**
MAST	Stramenopiles	Outside	0.535	0.001***
Chrysophyceae-Synurophyceae	Stramenopiles	Outside	0.516	0.002**
Katablepharidaceae	Hacrobia	Outside	0.505	0.001***
Pelagophyceae	Stramenopiles	Outside	0.470	0.002**
Bolidophyceae-and-relatives	Stramenopiles	Outside	0.402	0.012*
Spirotrichea	Alveolata	Outside	0.355	0.045*

Note: Only the top 50 phyla were included in the analysis and only phyla selected as significant ( $p < 0.05$ ) indicators are listed.

\*\*\* $p < 0.001$ ; \*\* $p < 0.01$ ; \* $p < 0.05$ .

## Photophysiology of the protist community and their changes across the meander

To examine whether these changes in community structure influence biological processes across the mesoscale meander, we investigated photophysiology using PAM fluorimetry. Overall, the photosynthetic efficiency of photosystem II (Fv/Fm) was significantly higher at the DCM compared with the surface ( $0.58 \pm 0.05$  and  $0.53 \pm 0.07$ , respectively;  $p < 0.01$ ). ETR and NPQ were not different between the surface and the DCM, although NPQ was negatively correlated with depth when excluding surface values (Table 2).

We observed significant differences in the photophysiology of the community across the meander. Fv/Fm was not significantly different between regions (Figure 6A), but ETR was significantly higher on the outside of the meander compared with the centre ( $31.95 \pm 6.81$  and  $25.48 \pm 6.23$ , respectively; Figure 6B). NPQ was significantly higher in the meander centre ( $0.36 \pm 0.12$ ) compared with the outside ( $0.19 \pm 0.07$ ) and the boundary ( $0.25 \pm 0.11$ ; Figure 6C).

To examine these differences in more detail, we determined correlations between photosynthetic parameters and environmental variables, both at the surface and at the DCM (Table 2).

Characteristics of the meander centre, i.e. lower temperature and salinity, higher chlorophyll fluorescence (Fo), and higher dO<sub>2</sub>, DIN, and phosphate were negatively correlated with Fv/Fm and ETR, and positively correlated with NPQ (except dO<sub>2</sub>, DIN with no

correlation). Thus, significant changes in photophysiology occur at a range of spatial scales across the meander. Note that these relationships do not always apply for both depths.

## Relationship between photophysiology, community diversity, and specific protist groups

Community Fv/Fm was negatively correlated to relative abundance of Haptophyta, and in particular the Prymnesiophyceae ( $R^2 = 0.22$ ,  $p < 0.0001$ ). The species driving this trend are ASV\_233 *Phaeocystis cordata* ( $R^2 = 0.14$ ,  $p < 0.01$ ), ASV\_60 *Prymnesiaceaea* spp. ( $R^2 = 0.14$ ,  $p < 0.01$ ), and ASV\_191 *Chrysochromulina\_X* ( $R^2 = 0.13$ ,  $p < 0.01$ ). Additional correlations with low community Fv/Fm are seen with high relative abundances of the chlorophytes Pyramimonadales and Prasino-Clade-7 ( $R^2 = 0.14$ ,  $p < 0.01$  for both).

In turn, high community Fv/Fm is primarily correlated to relative high abundances of Radiolaria, especially the groups RAD-B ( $R^2 = 0.3$ ,  $p < 0.0001$ ), and RAD-C ( $R^2 = 0.12$ ,  $p < 0.05$ ); the phylum Euglenozoa of the Discoba division and particularly ASV\_388 *Diplonema* spp. ( $R^2 = 0.26$ ,  $p < 0.0001$ ); and the chlorophytes Mamiellophyceae and particularly ASV\_337 *Micromonas* spp. ( $R^2 = 0.22$ ,  $p < 0.001$ ). Radiolarians are a non-plastidic heterotrophic clade commonly forming symbiotic relationships with photosynthetic taxa (Mars Brisbin et al., 2018).

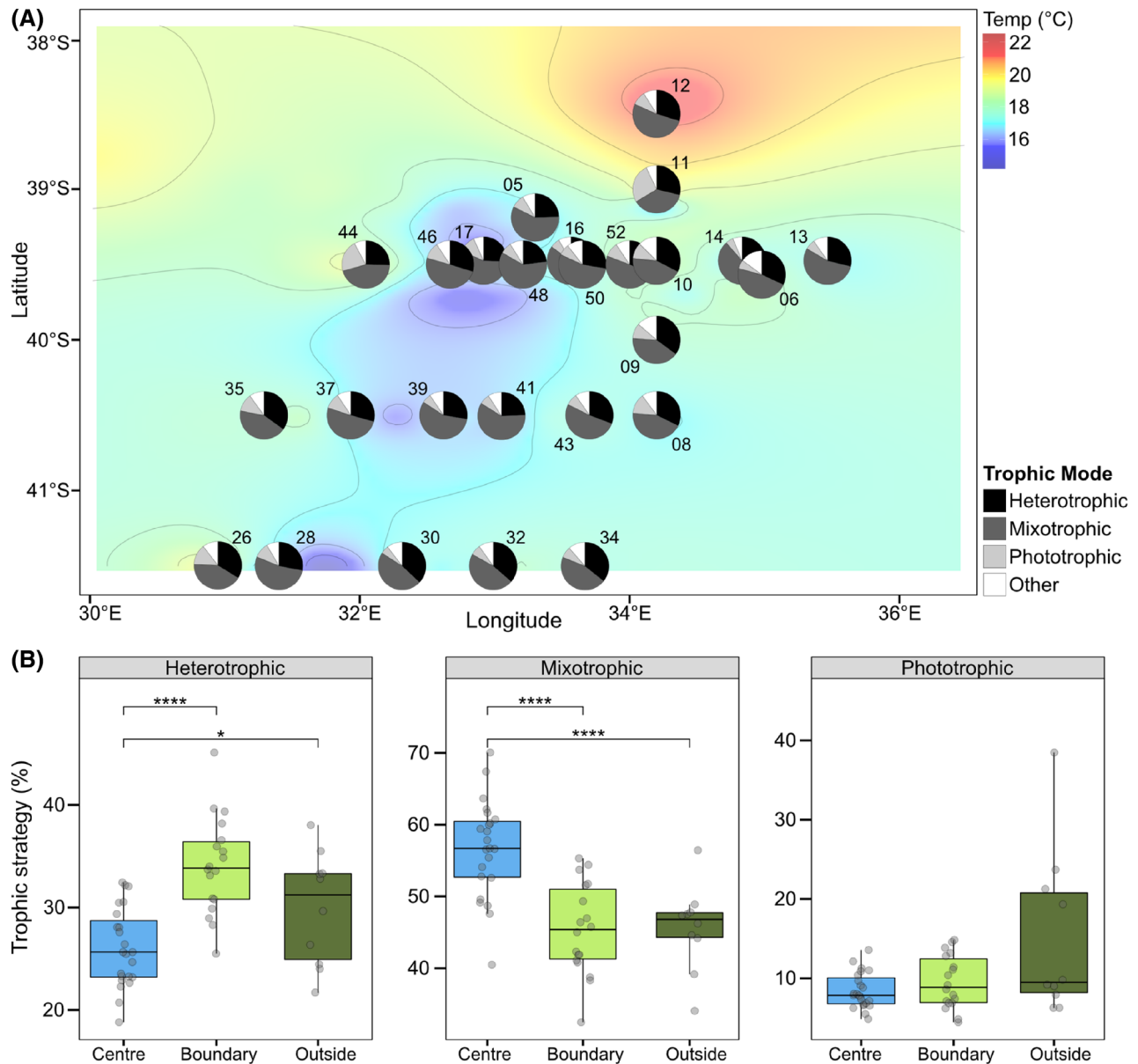


**FIGURE 4** Trophic structure of protist communities across the meander. (A) Trophic structure of protist communities overlaid on the temperature profile of the Subtropical Front meander. Piecharts are made up of the proportions heterotrophic (black), mixotrophic (dark grey), and phototrophic (light grey) clades, with white depicting clades which are unassigned. Proportions were summarized for surface and deep-chlorophyll maximum. (B) Trophic structure divided by trophic mode across the meander locations. Grey dots represent individual samples, boxplot centre lines represent median, box hinges indicate Quartiles 1 and 3, and whiskers 1.5 Interquartile Range from hinge or furthest data point, whichever is closer. Means between groups were compared using Wilcoxon rank-sum test. \*\*\*\* $p < 0.0001$ , \*\*\* $p < 0.001$ , \*\* $p < 0.01$ , \* $p < 0.05$ .

## Single-cell fluorimetry shows high variability of natural phytoplankton populations

Analyses at the community level show that photophysiology changes between the different regions of the meander. In an attempt to determine whether these differences are due to changes in physiology or community composition, we examined the photophysiology of single cells using PAM microscopy. We selected three

taxa for this analysis (dinoflagellates, diatoms, and coccolithophores) that could be readily identified by light microscopy and were abundant in most microscopy samples.

PAM microscopy was performed on phytoplankton samples from 12 stations, representing centre (8), boundary (2), and outside (2) of the meander. Combined mean single-cell values of Fv/Fm from all taxa (diatoms, coccolithophores, and dinoflagellates) were not significantly different from community Fv/Fm,

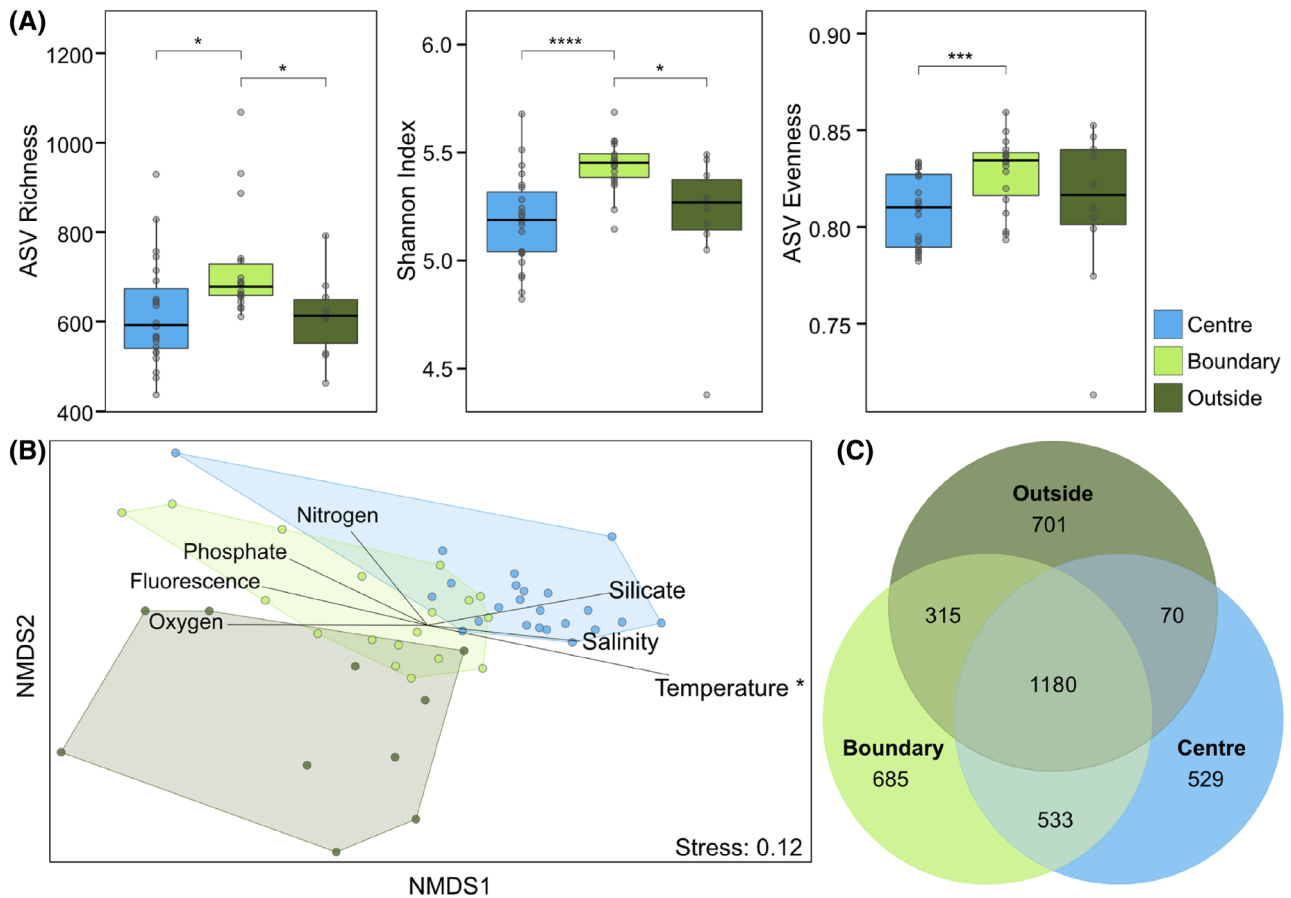


**FIGURE 5** Protist diversity across the meander (A) amplicon sequence variant (ASV) Richness, Shannon Index, and ASV Evenness at the meander locations. Boxplot centre lines represent median, box hinges indicate Quartiles 1 and 3, and whiskers 1.5 Interquartile Range from hinge or furthest data point, whichever is closer. Means between groups were compared using Wilcoxon rank-sum test: \*\*\* $p < 0.0001$ , \*\* $p < 0.001$ , \* $p < 0.01$ ,  $p < 0.05$ . (B) Non-metric multidimensional scaling ordination based on Bray–Curtis dissimilarity of protist community composition at the meander locations. Convex hull polygons delineate the three locations across the meander. Vector length and direction correspond to relative size effect and correlation to each axis, respectively. Temperature was the only significant ( $p < 0.05$  \*) environmental variable predicting community structure according to envfit analysis. (C) Venn-Diagram of shared ASVs between the meander locations. Colours: centre (blue), boundary (light green), and outside (dark green). Dots represent individual samples.

indicating that the two differing methodologies generated similar results (Figure S1A,  $p = 0.051$ ). Overall, mean Fv/Fm of dinoflagellates was significantly higher than mean Fv/Fm of coccolithophore cells (mean  $0.62 \pm 0.17$  and  $0.52 \pm 0.14$ , respectively; Figure 7A). Mean Fv/Fm of diatom cells was intermediate between coccolithophore and dinoflagellate values and was not significantly different to either (mean  $0.59 \pm 0.13$ ). There was no significant difference between the mean Fv/Fm values for small coccolithophores (i.e., *Emiliania Gephyrocapsa*) and other larger coccolithophore species (Figure 7A).

Overall, single-cell Fv/Fm values exhibited substantial variability within groups and across stations (Figure S1B). High variability between cells combined with low cell numbers for some taxa in certain samples limited our ability to compare single cell Fv/Fm values between taxa at individual stations. However, in samples where greater replication was achieved ( $n > 27$ ),

we did identify significant differences between taxa. For example, mean dinoflagellate Fv/Fm was significantly higher than coccolithophore Fv/Fm at Station 50 in the centre of the meander (mean  $0.65 \pm 0.17$  and  $0.49 \pm 0.14$ , respectively; Figure 7A). Examination of coccolithophore Fv/Fm values across the meander revealed significant differences between stations, although there was no consistent trend in the mean values between the three regions (centre, boundary, and outside; Figure S1B).

As lower community Fv/Fm values were associated with higher relative abundances of Prymnesiophyceae, we examined whether coccolithophores could be driving this trend. However, only four ASVs from metabarcoding were assigned to coccolithophores (ASV\_32 *Braarudosphaera bigelowii*, ASV\_780 *Helicosphaera carteri*, ASV\_783 *Gephyrocapsa oceanica*, and ASV\_3381 Clade E) and their abundances were not significantly correlated with community Fv/Fm. Several

**TABLE 2** Spearman correlations between photosynthetic parameters and environmental variables.

		Fv/Fm	ETR	NPQ
Overall	Depth (m)	0.37****	—	—
Surface		0.33**	—	—
DCM		0.21*	—	0.35**
Overall	Salinity	—	0.17**	0.17**
Surface		—	0.29**	—
DCM		0.22*	—	0.23**
Overall	Temperature	—	0.34****	—
Surface		—	0.32**	0.18*
DCM		0.15*	0.3**	—
Overall	dO <sub>2</sub>	0.16**	0.15**	—
Surface		—	0.3**	—
DCM		0.4****;	—	—
Overall	DIN	—	0.37****	—
Surface		—	0.43****	—
DCM		0.27**	—	—
Overall	Phosphate	—	0.25****	—
Surface		—	0.26**	0.2*
DCM		0.33**	0.15*	—
Overall	Silicate	—	—	—
Surface		—	0.25*	—
DCM		—	—	0.23*
Overall	Chl Fluorescence	—	0.26****	0.1*
Surface		—	0.44****	—
DCM		0.31**	0.17*	—
Overall	PAR	—	0.22***	—
Surface		—	—	—
DCM		—	—	—

Note: Results are shown for combined depths, and split by surface and DCM. Only significant correlations are represented where  $R^2 > 0.1$  and  $p < 0.05$ . Blue indicated a positive relationship, red an inverse relationship. Abbreviations: DCM, deep-chlorophyll maximum; DIN, dissolved inorganic nitrogen; ETR, electron transport rate; Fv/Fm, maximum quantum yield of photosystem II; NPQ, non-photochemical quenching. \*\*\*\* $p < 0.0001$ ; \*\*\* $p < 0.001$ ; \*\* $p < 0.01$ ; \* $p < 0.05$ .

ASVs which were not taxonomically assigned below phylum level did correlate negatively with Fv/Fm ( $R^2 = 0.13$ ,  $p < 0.05$ ).

### Single-cell PAM of cultured strains

Our single cell measurements of Fv/Fm in environmental populations of diatoms, dinoflagellates, and coccolithophores were characterized by high variability between cells. To investigate whether this was due to environmental stressors or species-specific differences, we performed single cell PAM microscopy on a range of laboratory grown phytoplankton cultures. We found that mean Fv/Fm values were significantly different between these taxa, being highest in dinoflagellates

(mean  $0.60 \pm 0.05$ ), lowest in haptophytes (mean  $0.51 \pm 0.08$ ), and with diatoms representing an intermediate value (mean  $0.56 \pm 0.04$ ; Wilcoxon,  $p < 0.001$ ; Figure 7B,C). Within each group, we found small but significant differences in the mean Fv/Fm values between most species, with low variability within each species. The standard deviation from mean Fv/Fm for all combined environmental samples was substantially greater (0.15) than for all investigated culture strains (0.06).

### DISCUSSION

Our study provides a comprehensive description of protist communities within a Southern Indian Ocean STF mesoscale meander using high-throughput environmental sequencing. This region is severely understudied despite its importance as a transition zone between the Indian and the Southern Ocean (Hood et al., 2017; Tripathy et al., 2017). Very few large-scale protist metabarcoding studies have sampled the SIO in detail, and even fewer local studies have chosen this area as their focus. This approach allowed us to characterize key protist groups in this region, as well as elucidating the drivers of diversity and trophic shifts in meander systems.

The use of 18S V9 metabarcoding suggests that the protist community in the study area of the SIO was dominated by the Alveolata, with over 70% of ASVs assigned to this clade. A similar community composition was also described for the Kerguelen area of the SO with nearly 70% of OTUs assigned to Alveolata (Georges et al., 2014). A sample site from the Tara Oceans expedition in close proximity to the study area was also dominated by Alveolata (42% in the 0.8–5  $\mu\text{m}$  DCM fraction, primarily Dinophyceae and the Syndiniales), followed by the Stramenopiles, Rhizarians and Hacrobia (De Vargas et al., 2015).

Potential caveats of metabarcoding are the capture of metabolically inactive organisms in a senescent state, as well as the introduction of biases through sample processing, primer choice, along with amplification and copy number bias (Santoferrara et al., 2020). The latter is of particular concern when examining dinoflagellate abundance, due to their multiple copies of small-subunit rDNA. Species with high copy numbers, such as ciliates and dinoflagellates, are therefore favoured, resulting in a lower relative abundance for other clades (Obiol et al., 2020). A further caveat in the use of 18S V9 metabarcoding comes from the observation that although the sampled area is part of the coccolithophore-rich Great Calcite Belt (Balch et al., 2016) and multiple coccolithophore species were observed in the single cell imaging studies, only four coccolithophore ASVs were identified with metabarcoding. Examination of the South Atlantic and South Indian

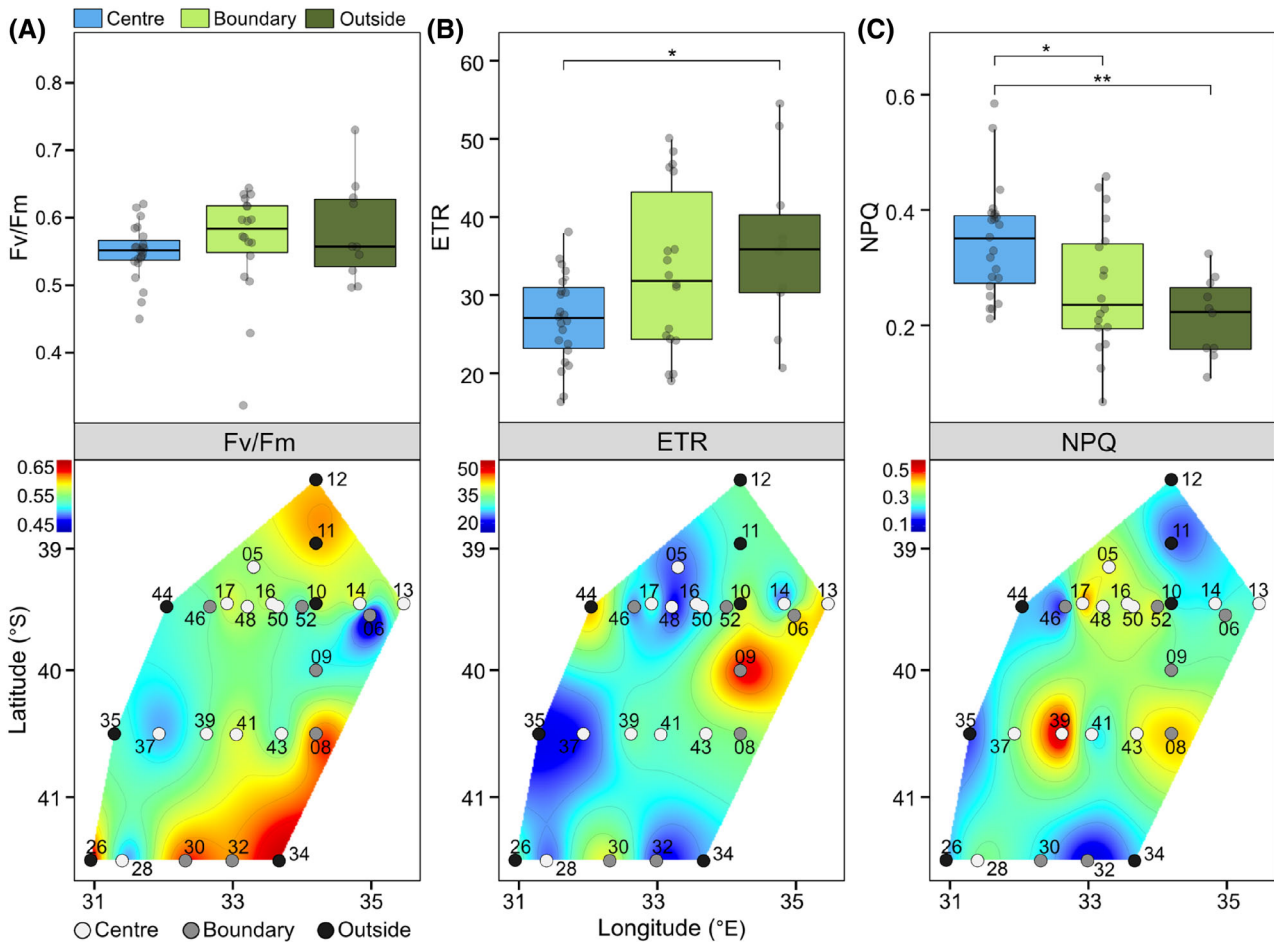


**FIGURE 6** Photophysiology of the protist community across the meander. (A) Maximum quantum yield of photosystem II (Fv/Fm), (B) electron transport rate (ETR), (C) non-photochemical quenching (NPQ) at the meander locations (top) and across the whole meander (bottom). Boxplot centre lines represent median, box hinges indicate Quartiles 1 and 3, and whiskers 1.5 Interquartile Range from hinge or furthest data point, whichever is closer. Grey dots represent individual samples. Means between groups were compared using Wilcoxon rank-sum test: \*\*\*\* $p < 0.0001$ , \*\*\* $p < 0.001$ , \*\* $p < 0.01$ , \* $p < 0.05$ .

sector of the Great Calcite Belt using SEM approaches identified up to 28 coccolithophore species, with *Emiliania huxleyi*, *Umbellosphaera tenuis*, *Syracosphaera* spp., and *Gephyrocapsa* spp. being the most abundant (Patil et al., 2020; Smith et al., 2017). Only the latter species was present in our 18S V9 metabarcoding dataset. The limitations of broad-range 18S Eukaryote primers for the detection of coccolithophores in metabarcoding studies have been described previously (Edvardsen et al., 2016) and 18S sequences are not yet available for many coccolithophore species. The development of improved primers (Egge et al., 2021), gene number correction factors (Martin et al., 2022), and using multiphasic approaches such as cell counts and PCR to help normalize disproportions are required to better understand these biases and their influence on the study of marine microbial communities.

We also found low relative abundances of diatoms in our metabarcoding analysis. Previous studies have reported a discrepancy between molecular methods

and light microscopy, where diatoms were underrepresented using high-throughput sequencing (Medinger et al., 2010; Gran-Stadniczeňko et al., 2019). However, it is known that diatom abundances in the SO decline north of the polar front due to lower silicon availability (Balch et al., 2016; Smith et al., 2017).

Notwithstanding the above caveats, examination of the protist community across the STF mesoscale meander indicated that diversity was greatest at the boundary. Increased community diversity at the Agulhas frontal boundary has previously been identified in bacterioplankton through 16S rRNA gene amplicon and metagenomic sequencing (Phoma et al., 2018). Frontal boundaries in subtropical and subantarctic waters near New Zealand were also identified as bacterioplankton diversity hotspots, although no such effect was observed on protist communities (Allen et al., 2020). However, higher chlorophyll *a* concentrations and primary production rates have previously been found at the periphery of an eddy system in the eastern tropical

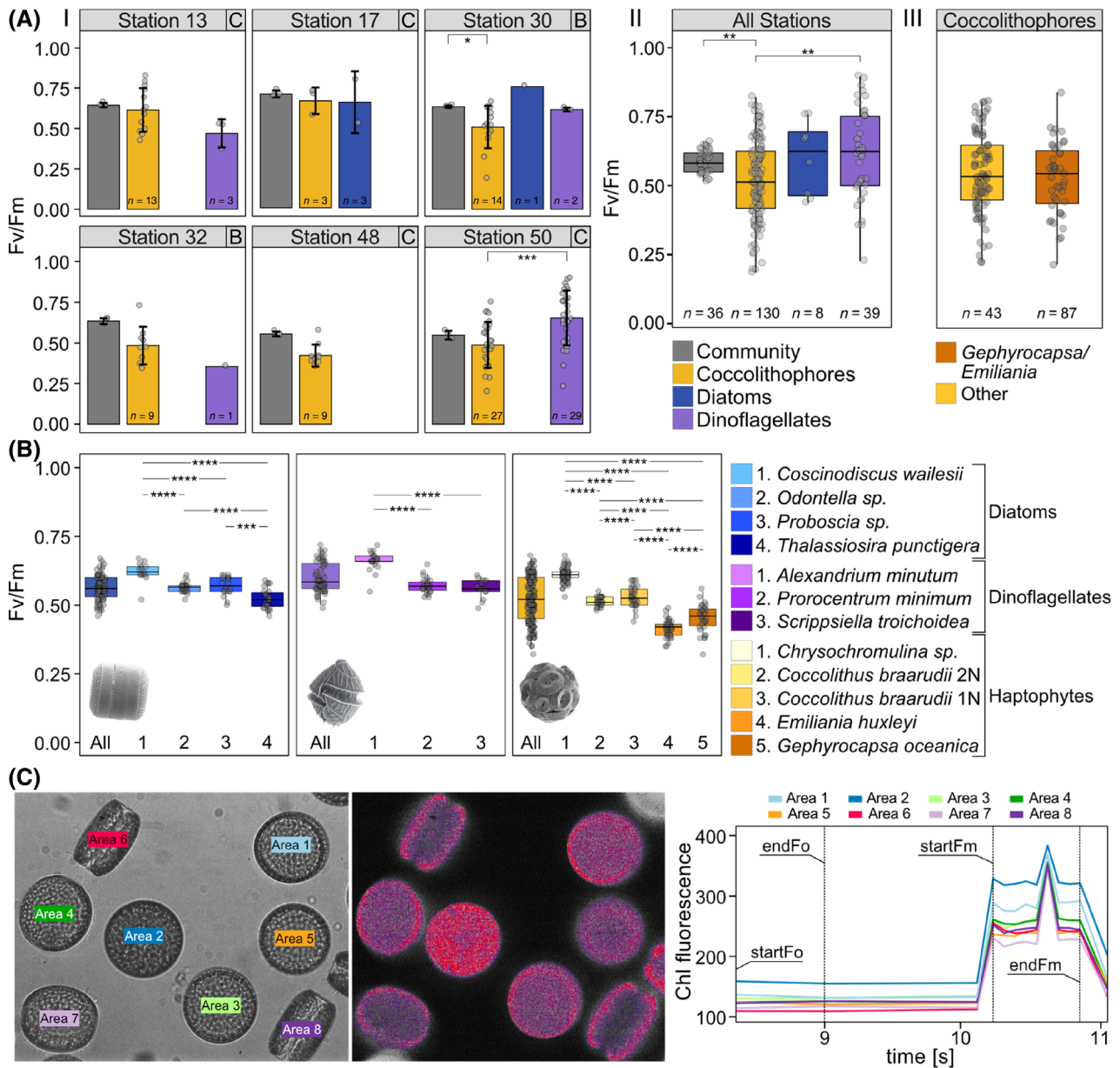


**FIGURE 7** Photophysiology of environmental phytoplankton populations and laboratory monocultures obtained with single-cell pulse amplitude modulated (PAM) microscopy (A) Results from single-cell PAM microscopy (colours) for coccolithophores, dinoflagellates, and diatoms as well as community Fv/Fm from water-PAM (grey). I: Fv/Fm for selected stations, barplots show mean ± SD. Boxes in the top right corner of each panel indicate the respective meander location: C, Centre; B, Boundary. II: Fv/Fm for all surveyed stations combined. III: Single-cell coccolithophore Fv/Fm divided by *Emiliania*/*Gephyrocapsa* and Others. (B) Fv/Fm distributions for laboratory monocultures obtained with single-cell PAM microscopy (all measurements within a group and measurements within species). Boxplot centre lines represent median, box hinges indicate Quartiles 1 and 3, and whiskers 1.5 Interquartile Range from hinge or furthest data point, whichever is closer. Means between groups were compared using Wilcoxon rank-sum test: \*\*\*\* $p < 0.0001$ , \*\*\* $p < 0.001$ , \*\* $p < 0.01$ , \* $p < 0.05$ . Dots represent individual samples. (C) Example of representative single-cell PAM fluorescence imaging of diatom *Thalassiosira punctigera*. Left: bright field image of selected cells (region of interest [ROI] was drawn around each cell) and respective area within ROI where chlorophyll fluorescence is measured Middle: Chlorophyll fluorescence (Fo), Right: fluorescence plots of dark-adapted state Fo, followed by a saturating light pulse Fm for each selected area. Average Fm signal is calculated between checkpoints StartFm and EndFm.

north Atlantic (Devresse et al., 2022). The meander was defined by substantial gradients in temperature and salinity, with salinity barriers identified as one of the strongest factors shaping protist communities in marine environments (Singer et al., 2021). Local oceanic features, such as the meander investigated in this

study, can therefore underlie shifts in protist communities even over short distances (Burki et al., 2021).

The process responsible for enhanced satellite-derived chlorophyll within SIO mesoscale eddies may be horizontal advection of nutrient-rich waters and deeper convective mixing of the DCM (Dufois et al., 2017).

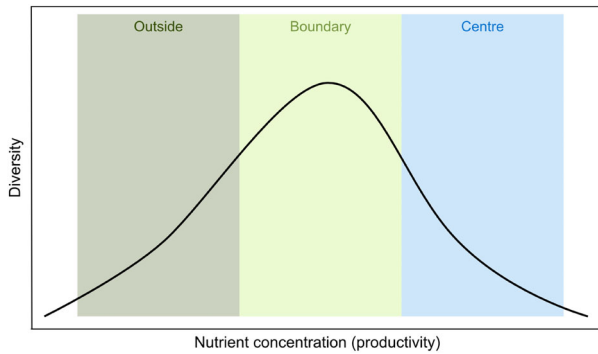


**FIGURE 8** Proposed schematic of the meander regions on the bell-shaped Productivity/Diversity curve. Protist community peaks at medium nutrient concentrations while single clades may outcompete others in high-nutrient environments.

Nutrients were higher at the centre of the meander and lower outside. Peak diversity at the meander boundary could therefore be explained by the bell-shaped Productivity/Diversity Relationship (Kassen et al., 2000; Vallina et al., 2014), which suggests decreasing diversity in a region where nutrient concentrations are high enough for specific clades to dominate. This effect is also found in the DARWIN ocean-ecosystem model, with increased group and intra-group diversity in frontal regions (based on Shannon index), which was more pronounced for the lower nutrient subtropical front than the higher nutrient subpolar front (Mangolte et al., 2022). The frontal system of the STF meander investigated in this study could therefore contain a ‘sweet spot’ of nutrient concentrations for a balanced and diverse protist community (Figure 8).

The change in diversity across the meander was associated with a clear transition in community structure as inferred from Bray–Curtis dissimilarity, as well as trophic structure. The dominating trophic mode in the meander centre was mixotrophy, likely due to the relatively higher abundance of Dinophyceae in this environment. The trophic balance within a mesoscale eddy can shift from phototrophy to heterotrophy within a few weeks (Mourino-Carballido & McGillicuddy Jr, 2006). We show that several modes of nutrition can occur within a single mesoscale meander, highlighting the complexity of microbial metabolic activity dynamics within such features. This is in accordance with a previous study investigating trophic variability within a cyclonic eddy of the tropical north Atlantic (Devresse et al., 2022).

Heterotrophic taxa increased in abundance at the meander boundary, including the parasitic Syndiniales (Alveolata) as well as multiple Rhizarian groups (Acantharea, Polycystinea, and RAD-C). Ocean-Ecosystem modelling suggested that diatoms, dinoflagellates, and large carnivorous zooplankton benefit most from frontal environments, while coccolithophores and pico-phytoplankton groups and small grazers also

increase but are less favoured (Mangolte et al., 2022). The modelling study proposed that nutrient enrichment may enhance the prevalence of fast-growing plankton groups. Additionally, motile species with the ability for vertical migration, thus taking advantage of multiple water types with different nutrient concentrations, are likely more competitive in stratified environments.

We also observed broad scale changes in the photophysiology of the phytoplankton communities. Community Fv/Fm was higher at the DCM compared with the surface. When all depths were considered, Fv/Fm did not change across the meander regions, although we did observe elevated NPQ and highest chlorophyll fluorescence (Fo: a proxy for phytoplankton abundance) at the meander centre and higher ETR outside of the meander. Lower Fv/Fm in surface waters could be due to lower nutrients and/or higher irradiance in surface waters (Li & Hansell, 2008; Rii et al., 2008), although changes in community composition could also contribute. By performing a meta-analysis of in situ experiments combined with measurements of laboratory cultures, Suggett et al. (2009) concluded that changes in photophysiology due to nutrient limitation were often likely to be outweighed by changes in community composition, except in severely Fe-limited waters.

Low Fv/Fm values at individual stations correlated with a higher relative abundance of haptophytes in our metabarcoding analysis, specifically the Prymnesiophyceae. Furthermore, our single-cell imaging PAM data indicated that coccolithophore (Class Prymnesiophyceae) Fv/Fm was significantly lower than community Fv/Fm. Together these results suggest that an increase in the abundance of haptophytes could be driving the changes in community photophysiology. However, support for this hypothesis from the metabarcoding data is not strong. The Prymnesiophyceae only represented a minor proportion of the protist community (2.7% of total), although they do represent a higher proportion of the photosynthetic taxa present. Moreover, of the four identified coccolithophore ASVs, none were associated with low community Fv/Fm. However, some of the Prymnesiophyceae ASVs which were not taxonomically assigned below phylum level may represent coccolithophore taxa for which no associated 18S reference sequence yet exists. Further analyses are needed, in particular the assessment of haptophyte abundance through other approaches, to examine whether they are driving the changes in photophysiology.

Our study highlights some of the important issues, such as the under- and over-representation of certain taxa, which need to be considered when using metabarcoding data to assess relationships between community structure and function. It should also be noted that 18S rDNA metabarcoding excludes photosynthetic prokaryotes (i.e., cyanobacteria), which often have a

relatively low Fv/Fm compared with photosynthetic eukaryotes (Suggett et al., 2009). Cyanobacteria are not expected to be dominant primary producers within the phytoplankton communities of the Southern Ocean, but this may be an important consideration for other study areas, such as the oligotrophic open oceans where unicellular cyanobacteria dominate (Hagström et al., 1988).

Here, we demonstrate that it is possible to directly measure the photosynthetic efficiency of single identified phytoplankton cells from environmental populations on a research vessel. Moreover, trends in our environmental dataset of lower haptophyte Fv/Fm relative to dinoflagellates were supported by subsequent studies of laboratory cultures. These findings show that PAM microscopy can be used to assess the photophysiology of individual taxa within natural phytoplankton populations. However, whilst we were able to observe trends between taxa using combined measurements, only a few individual stations exhibited significant differences between taxa, due largely to the very high variability in Fv/Fm values in individual cells from natural populations. These ranged from <0.2 to >0.8, close to the theoretical maximum for PSII. We were able to replicate ocean temperature precisely throughout these measurements, so the variability was not a result of temperature stress during the analysis. Previous studies report maximum Fv/Fm values of 0.65 for phytoplankton in nutrient replete environments (Kolber & Falkowski, 1993), while values of <0.4 indicate iron-stressed phytoplankton in the SO (Boyd & Abraham, 2001; Kerkar et al., 2020). Our results reveal a much greater diversity in Fv/Fm values in individual cells that are not apparent in population-level measurements. In laboratory monoculture, we showed that nearly all investigated haptophyte species were significantly different from one another with very little variability within species. The same trend was evident for dinoflagellates and diatoms. Overall, differences between species only explained a small proportion of the variability we saw in environmental populations. Environmental stressors such as nutrient or light limitation, growth phase, or competition are therefore likely bigger contributors to the observed variability in photosynthetic efficiency than species-specific differences. Interestingly, this conclusion differs from Suggett et al., 2009, who found that alleviation of nutrient limitation had a lower impact on community photophysiology than a shift in community structure, except in iron-limited populations, such as is likely in the SIO. Clearly, many more measurements of natural populations are needed to understand how variability at the single-cell level could influence the photophysiology of the population as a whole.

In summary, we show that the mesoscale meander features in the Southern Indian Ocean have significant impacts on community composition and function (in terms of photosynthetic parameters), with the increased diversity at the boundary of the meander

indicative of a unique environment for protist communities. These data highlight the importance of mesoscale phenomena for biological processes, by not only trapping and transporting nutrients but also stimulating growth of photo- and heterotrophic protists. Given that the dominant trophic strategy of ecological systems influences carbon fate, mesoscale meanders and eddies may be important factors in altering local carbon cycling, as well as carrying productive phototrophic systems into otherwise oligotrophic, low-productivity regions.

## AUTHOR CONTRIBUTIONS

**Daniela Sturm:** Conceptualization (lead); data curation (lead); formal analysis (lead); funding acquisition (supporting); investigation (lead); methodology (lead); project administration (lead); validation (lead); visualization (lead); writing – original draft (lead); writing – review and editing (lead). **Joost de Vries:** Data curation (supporting); writing – review and editing (supporting). **William M. Balch:** Funding acquisition (supporting); project administration (supporting); writing – review and editing (supporting). **Glen Wheeler:** Conceptualization (supporting); funding acquisition (supporting); project administration (supporting); supervision (lead); writing – original draft (supporting); writing – review and editing (supporting). **Colin Brownlee:** Data curation (supporting); formal analysis (supporting); funding acquisition (supporting); project administration (equal); supervision (equal); writing – review and editing (supporting).

## ACKNOWLEDGEMENTS

The authors thank the crew and technical staff on R/V *Thomas Thompson* as well as the scientists that participated in sample acquisition and equipment installation onboard.

## FUNDING INFORMATION

This work was supported by a European Research Council Advanced Grant (ERC-ADG-670390) and the Leverhulme Trust (EM-2021-067) to Colin Brownlee, Natural Environmental Research Council INSPIRE Doctoral Training Program (NE/SO07210/1), and National Science Foundation (NSF) grant OCE-1735664 (William M. Balch).

## CONFLICT OF INTEREST STATEMENT

The authors declare that the research was conducted in the absence of any commercial or financial relationships that could be construed as a potential conflict of interest.

## DATA AVAILABILITY STATEMENT

Raw sequencing reads are deposited in the Sequence Read Archive (SRA) (Accession PRJNA952565). All data will be made available following publication.



## ORCID

Daniela Sturm  <https://orcid.org/0000-0001-7395-6781>

## REFERENCES

- Allen, R., Summerfield, T.C., Currie, K., Dillingham, P.W. & Hoffmann, L.J. (2020) Distinct processes structure bacterioplankton and protist communities across an oceanic front. *Aquatic Microbial Ecology*, 85, 19–34.
- Alory, G., Wijffels, S. & Meyers, G. (2007) Observed temperature trends in the Indian Ocean over 1960–1999 and associated mechanisms. *Geophysical Research Letters*, 34, 34.
- Amaral-Zettler, L.A., McCliment, E.A., Ducklow, H.W. & Huse, S.M. (2009) A method for studying protistan diversity using massively parallel sequencing of V9 hypervariable regions of small-subunit ribosomal RNA genes. *PLoS One*, 4, e6372.
- Anderson, M.J. (2001) A new method for non-parametric multivariate analysis of variance. *Austral Ecology*, 26, 32–46.
- Arrigo, K.R., van Dijken, G.L. & Bushinsky, S. (2008) Primary production in the Southern Ocean, 1997–2006. *Journal of Geophysical Research: Oceans*, 113, C08004.
- Atlas, E.L., Hager, S.W., Gordon, L.I. & Park, P.K. (1971) *A practical manual for use of the Technicon AutoAnalyzer® in seawater nutrient analyses revised*. Technical Report 215. Oregon State University, Department of Oceanography.
- Balch, W.M., Bates, N.R., Lam, P.J., Twining, B.S., Rosengard, S.Z., Bowler, B.C. et al. (2016) Factors regulating the great Calcite Belt in the Southern Ocean and its biogeochemical significance. *Global Biogeochemical Cycles*, 30, 1124–1144.
- Belkin, N., Guy-Haim, T., Rubin-Blum, M., Lazar, A., Sisma-Ventura, G., Kiko, R. et al. (2022) Influence of cyclonic and anti-cyclonic eddies on plankton in the southeastern Mediterranean Sea during late summertime. *Ocean Science*, 18, 693–715.
- Blanco-Bercial, L., Parsons, R., Bolanos, L., Johnson, R., Giovannoni, S. & Curry, R. (2022) The protist community mirrors seasonality and mesoscale hydrographic features in the oligotrophic Sargasso Sea. Authorea Prepr. <https://www.authorea.com/users/453879/articles/551657-the-protist-community-mirrors-seasonality-and-mesoscale-hydrographic-features-in-the-oligo-trophic-sargasso-sea>
- Boyd, P.W. & Abraham, E.R. (2001) Iron-mediated changes in phytoplankton photosynthetic competence during SOIREE. *Deep Sea Research Part II: Topical Studies in Oceanography*, 48, 2529–2550.
- Bradley, I.M., Pinto, A.J. & Guest, J.S. (2016) Design and evaluation of Illumina MiSeq-compatible, 18S rRNA gene-specific primers for improved characterization of mixed phototrophic communities. *Applied and Environmental Microbiology*, 82, 5878–5891.
- Burki, F., Sandin, M.M. & Jamy, M. (2021) Diversity and ecology of protists revealed by metabarcoding. *Current Biology*, 31, R1267–R1280.
- Callahan, B.J., McMurdie, P.J., Rosen, M.J., Han, A.W., Johnson, A.J.A. & Holmes, S.P. (2016) DADA2: high-resolution sample inference from Illumina amplicon data. *Nature Methods*, 13, 581–583.
- Caron, D.A., Worden, A.Z., Countway, P.D., Demir, E. & Heidelberg, K.B. (2009) Protists are microbes too: a perspective. *The ISME Journal*, 3, 4–12.
- Catlett, D., Matson, P.G., Carlson, C.A., Wilbanks, E.G., Siegel, D.A. & Iglesias-Rodriguez, M.D. (2020) Evaluation of accuracy and precision in an amplicon sequencing workflow for marine protist communities. *Limnology and Oceanography: Methods*, 18, 20–40.
- Christaki, U., Georges, C., Genitsaris, S. & Monchy, S. (2015) Microzooplankton community associated with phytoplankton blooms in the naturally iron-fertilized Kerguelen area (Southern Ocean). *FEMS Microbiology Ecology*, 91, fiv068.
- Christaki, U., Skouroliakou, I.D., Delegrange, A., Irion, S., Courcot, L., Jardillier, L. et al. (2021) Microzooplankton diversity and potential role in carbon cycling of contrasting Southern Ocean productivity regimes. *Journal of Marine Systems*, 219, 103531.
- Countway, P.D., Caron, D.A., Gast, R.J. & Savai, P. (2007) Comparison of protistan diversity in deep (2500 m) vs euphotic zone assemblages in the Sargasso Sea and Gulf Stream (N. Atlantic). *Environmental Microbiology*, 9, 1219–1232.
- De Vargas, C., Audic, S., Henry, N., Decelle, J., Mahé, F. & Logares, R. (2015) Eukaryotic plankton diversity in the sunlit ocean. *Science*, 348, 1261605.
- Devresse, Q., Becker, K.W., Bendinger, A., Hahn, J. & Engel, A. (2022) Eddy enhanced primary production accelerates bacterial growth in the eastern tropical North Atlantic. *Biogeosciences Discussions*, 2022, 1–41.
- Dufois, F., Hardman-Mountford, N.J., Fernandes, M., Wojtasiewicz, B., Shenoy, D., Slawinski, D. et al. (2017) Observational insights into chlorophyll distributions of subtropical South Indian Ocean eddies. *Geophysical Research Letters*, 44, 3255–3264.
- Dufréne, M. & Legendre, P. (1997) Species assemblages and indicator species: the need for a flexible asymmetrical approach. *Ecological Monographs*, 67, 345–366.
- Edvardsen, B., Egge, E.S. & Vulot, D. (2016) Diversity and distribution of haptophytes revealed by environmental sequencing and metabarcoding – a review. *Perspectives in Phycology*, 3, 77–91.
- Egge, E., Elferink, S., Vulot, D., John, U., Bratbak, G., Larsen, A. et al. (2021) An 18S V4 rDNA metabarcoding dataset of protist diversity in the Atlantic inflow to the Arctic Ocean, through the year and down to 1000 m depth. *Earth System Science Data Discussions*, 13, 4913–4928.
- El Lutjeharms, J.R. & Valentine, H.R. (1984) Southern Ocean thermal fronts south of Africa. *Deep Sea Research Part A. Oceanographic Research Papers*, 31, 1461–1475.
- Frölicher, T.L., Sarmiento, J.L., Paynter, D.J., Dunne, J.P., Krasting, J.P. & Winton, M. (2015) Dominance of the Southern Ocean in anthropogenic carbon and heat uptake in CMIP5 models. *Journal of Climate*, 28, 862–886.
- Georges, C., Monchy, S., Genitsaris, S. & Christaki, U. (2014) Protist community composition during early phytoplankton blooms in the naturally iron-fertilized Kerguelen area (Southern Ocean). *Biogeosciences*, 11, 5847–5863.
- Glover, D.M., Doney, S.C., Oestreich, W.K. & Tullo, A.W. (2018) Geostatistical analysis of mesoscale spatial variability and error in SeaWiFS and MODIS/aqua global ocean color data. *Journal of Geophysical Research: Oceans*, 123, 22–39.
- Gordon, A.L. (1967) In: Bushnell, V. (Ed.) *Structure of Antarctic waters between 20°W and 170°W, Antarctic Map Folio Series, folio 6*. New York: American Geographical Society.
- Gordon, L.I., Jennings, J.C., Jr., Ross, A.A. & Krest, J.M. (1993) A suggested protocol for continuous flow automated analysis of seawater nutrients (phosphate, nitrate, nitrite and silicic acid) in the WOCE hydrographic program and the joint Global Ocean fluxes study. *WOCE hydrographic program office, methods manual WHPO 68/91*, 1–52.
- Gran-Stadniczeňko, S., Egge, E., Hostyeva, V., Logares, R., Eikrem, W. & Edvardsen, B. (2019) Protist diversity and seasonal dynamics in Skagerrak plankton communities as revealed by metabarcoding and microscopy. *Journal of Eukaryotic Microbiology*, 66(3), 494–513.
- Guillard, R.R.L. (1975) Culture of phytoplankton for feeding marine invertebrates. *WOCE hydrographic program office, methods manual WHPO 68/91*. Springer, pp. 29–60.
- Guillou, L., Bachar, D., Audic, S., Bass, D., Berney, C., Bittner, L. et al. (2012) The Protist ribosomal reference database (PR2): a catalog of unicellular eukaryote small sub-unit rRNA sequences with curated taxonomy. *Nucleic Acids Research*, 41, D597–D604.

- Hager, S.W., Atlas, E.L., Gordon, L.I., Mantyla, A.W. & Park, P.K. (1972) A comparison at sea of manual and autoanalyzer analyses of phosphate, nitrate, and silicate. *Limnology and Oceanography*, 17, 931–937.
- Hagström, Å., Azam, F., Andersson, A., Wikner, J. & Rassoulzadegan, F. (1988) Microbial loop in an oligotrophic pelagic marine ecosystem: possible roles of cyanobacteria and nanoflagellates in the organic fluxes. *Marine Ecology Progress Series*, 49, 171–178.
- Hernández-Hernández, N., Arístegui, J., Montero, M.F., Velasco-Senovilla, E., Baltar, F., Marrero-Díaz, Á. et al. (2020) Drivers of plankton distribution across mesoscale eddies at submesoscale range. *Frontiers in Marine Science*, 7, 667.
- Hood, R.R., Beckley, L.E. & Wiggert, J.D. (2017) Biogeochemical and ecological impacts of boundary currents in the Indian Ocean. *Progress in Oceanography*, 156, 290–325.
- Kassen, R., Buckling, A., Bell, G. & Rainey, P.B. (2000) Diversity peaks at intermediate productivity in a laboratory microcosm. *Nature*, 406, 508–512.
- Kerker, A.U., Tripathy, S.C., Minu, P., Baranval, N., Sabu, P., Patra, S. et al. (2020) Variability in primary productivity and biological properties in the Indian sector of the Southern Ocean during an austral summer. *Polar Biology*, 43, 1469–1492.
- Kolber, Z. & Falkowski, P.G. (1993) Use of active fluorescence to estimate phytoplankton photosynthesis in situ. *Limnology and Oceanography*, 38, 1646–1665.
- Kromkamp, J.C. & Forster, R.M. (2003) The use of variable fluorescence measurements in aquatic ecosystems: differences between multiple and single turnover measuring protocols and suggested terminology. *European Journal of Phycology*, 38, 103–112.
- Landschützer, P., Gruber, N., Haumann, F.A., Rödenbeck, C., Bakker, D.C.E., Van Heuven, S. et al. (2015) The reinvigoration of the Southern Ocean carbon sink. *Science*, 349, 1221–1224.
- Lee, S., Wolberg, G. & Shin, S.Y. (1997) Scattered data interpolation with multilevel B-splines. *IEEE Transactions on Visualization and Computer Graphics*, 3, 228–244.
- Lehahn, Y., d'Ovidio, F., Lévy, M., Amitai, Y. & Heifetz, E. (2011) Long range transport of a quasi isolated chlorophyll patch by an Agulhas ring. *Geophysical Research Letters*, 38, L16610.
- Li, Q., England, M.H. & Hogg, A.M.C. (2021) Transient response of the Southern Ocean to idealized wind and thermal forcing across different model resolutions. *Journal of Climate*, 34, 5477–5496.
- Li, Q.P. & Hansell, D.A. (2008) Nutrient distributions in baroclinic eddies of the oligotrophic North Atlantic and inferred impacts on biology. *Deep Sea Research Part II: Topical Studies in Oceanography*, 55, 1291–1299.
- Longhurst, A. (1998) *Ecological geography of the sea*. San Diego: Academic Press, p. 398.
- Mangolte, I., Lévy, M., Dutkiewicz, S., Clayton, S., Mangolte, I., Lévy, M. et al. (2022) Plankton community response to fronts: winners and losers to cite this version: HAL id: HAL-03607937 plankton community response to fronts: winners and losers.
- Mars Brisbin, M., Mesrop, L.Y., Grossmann, M.M. & Mitarai, S. (2018) Intra-host symbiont diversity and extended symbiont maintenance in photosymbiotic *Acantharea* (clade F). *Frontiers in Microbiology*, 9, 1998.
- Martin, J.L., Santi, I., Pitta, P., John, U. & Gypens, N. (2022) Towards quantitative metabarcoding of eukaryotic plankton: an approach to improve 18S rRNA gene copy number bias. *Metabarcoding and Metagenomics*, 6, 245–259.
- Martin, M. (2011) Cutadapt removes adapter sequences from high-throughput sequencing reads. *EMBnet Journal*, 17, 10–12.
- McMurdie, P.J. & Holmes, S. (2013) Phyloseq: an R package for reproducible interactive analysis and graphics of microbiome census data. *PLoS One*, 8, e61217.
- Medinger, R., Nolte, V., Pandey, R.V., Jost, S., Ottenwälder, B., Schlötterer, C. & Boenigk, J. (2010) Diversity in a hidden world: potential and limitation of next-generation sequencing for surveys of molecular diversity of eukaryotic microorganisms. *Molecular Ecology*, 19, 32–40.
- Mitra, A., Flynn, K.J., Tillmann, U., Raven, J.A., Caron, D., Stoecker, D.K. et al. (2016) Defining planktonic protist functional groups on mechanisms for energy and nutrient acquisition: incorporation of diverse mixotrophic strategies. *Protist*, 167, 106–120.
- Moore, C.M., Suggett, D., Holligan, P.M., Sharples, J., Abraham, E.R., Lucas, M.I. et al. (2003) Physical controls on phytoplankton physiology and production at a shelf sea front: a fast repetition-rate fluorometer based field study. *Marine Ecology Progress Series*, 259, 29–45.
- Mourino-Carballido, B. & McGillicuddy, D.J., Jr. (2006) Mesoscale variability in the metabolic balance of the Sargasso Sea. *Limnology and Oceanography*, 51, 2675–2689.
- Obiol, A., Giner, C.R., Sánchez, P., Duarte, C.M., Acinas, S.G. & Massana, R. (2020) A metagenomic assessment of microbial eukaryotic diversity in the global ocean. *Molecular Ecology Resources*, 20, 718–731.
- Oxborough, K. (2004) Imaging of chlorophyll a fluorescence: theoretical and practical aspects of an emerging technique for the monitoring of photosynthetic performance. *Journal of Experimental Botany*, 55, 1195–1205.
- Patil, S.M., Mohan, R., Shetye, S.S., Gazi, S., Choudhari, P. & Jafar, S. (2020) Interannual changes of austral summer coccolithophore assemblages and southward expansion in the southern Indian Ocean. *Deep Sea Research Part II: Topical Studies in Oceanography*, 178, 104765.
- Petrou, K., Baker, K.G., Nielsen, D.A., Hancock, A.M., Schulz, K.G. & Davidson, A.T. (2019) Acidification diminishes diatom silica production in the Southern Ocean. *Nature Climate Change*, 9, 781–786.
- Phoma, S., Vikram, S., Jansson, J.K., Anson, I.J., Cowan, D.A., Van De Peer, Y. et al. (2018) Agulhas current properties shape microbial community diversity and potential functionality. *Scientific Reports*, 8, 1–12.
- Pingree, R.D., Holligan, P.M. & Mardell, G.T. (1979) Phytoplankton growth and cyclonic eddies. *Nature*, 278, 245–247.
- Pingree, R.D., Pugh, P.R., Holligan, P.I. & Forster, G.R. (1975) Summer phytoplankton blooms and red tides along tidal fronts in the approaches to the English Channel. *Nature*, 258, 672–677.
- Rembauville, M., Briggs, N., Ardyna, M., Uitz, J., Catala, P., Penker, C. et al. (2017) Plankton assemblage estimated with BGC-Argo floats in the Southern Ocean: implications for seasonal successions and particle export. *Journal of Geophysical Research: Oceans*, 122, 8278–8292.
- Rii, Y.M., Brown, S.L., Nencioli, F., Kuwahara, V., Dickey, T., Karl, D.M. et al. (2008) The transient oasis: nutrient-phytoplankton dynamics and particle export in Hawaiian lee cyclones. *Deep Sea Research Part II: Topical Studies in Oceanography*, 55, 1275–1290.
- Rouault, M., Penven, P. & Pohl, B. (2009) Warming in the Agulhas current system since the 1980's. *Geophysical Research Letters*, 36, L12602.
- Santoferrara, L., Burki, F., Filker, S., Logares, R., Dunthorn, M. & McManus, G.B. (2020) Perspectives from ten years of Protist studies by high-throughput metabarcoding. *The Journal of Eukaryotic Microbiology*, 67, 612–622.
- Sassenhagen, I., Irion, S., Jardillier, L., Moreira, D. & Christaki, U. (2020) Protist interactions and community structure during early autumn in the Kerguelen region (Southern Ocean). *Protist*, 171, 1–20.
- Singer, D., Seppey, C.V.W., Lentendu, G., Dunthorn, M., Bass, D., Belbahri, L. et al. (2021) Protist taxonomic and functional diversity in soil, freshwater and marine ecosystems. *Environment International*, 146, 106262.

- Smith, H.E.K., Poulton, A.J., Garley, R., Hopkins, J., Lubelczyk, L.C., Drapeau, D.T. et al. (2017) The influence of environmental variability on the biogeography of coccolithophores and diatoms in the Great Calcite Belt. *Biogeosciences*, 14, 4905–4925.
- Sturm, D., Langer, G. & Wheeler, G. (2022) Novel combination coccospores from *Helicosphaera* spp indicate complex relationships between species. *Journal of Plankton Research*, 44, 838.
- Suggett, D.J., Moore, C.M., Hickman, A.E. & Geider, R.J. (2009) Interpretation of fast repetition rate (FRR) fluorescence: signatures of phytoplankton community structure versus physiological state. *Marine Ecology Progress Series*, 376, 1–19.
- Suggett, D.J., Oxborough, K., Baker, N.R., MacIntyre, H.L., Kana, T.M. & Geider, R.J. (2003) Fast repetition rate and pulse amplitude modulation chlorophyll a fluorescence measurements for assessment of photosynthetic electron transport in marine phytoplankton. *European Journal of Phycology*, 38, 371–384.
- Tripathy, S.C., Mishra, R.K. & Naik, R.K. (2017) Progress in Southern Ocean biology from the Indian sector: half-decadal (2009–13) overview. *Proceedings of the Indian National Science Academy*, 83, 385–398.
- Vallina, S.M., Follows, M.J., Dutkiewicz, S., Montoya, J.M., Cermeno, P. & Loreau, M. (2014) Global relationship between phytoplankton diversity and productivity in the ocean. *Nature Communications*, 5, 4299.
- Weber, T.S. & Deutsch, C. (2010) Ocean nutrient ratios governed by plankton biogeography. *Nature*, 467, 550–554.
- Wickham, H., Chang, W. & Wickham, M.H. (2016) Package 'ggplot2'. *Create elegant data visualisations using the grammar of graphics. Version, 2*, 1–189.

## SUPPORTING INFORMATION

Additional supporting information can be found online in the Supporting Information section at the end of this article.

**How to cite this article:** Sturm, D., de Vries, J., Balch, W.M., Wheeler, G. & Brownlee, C. (2023) Mesoscale oceanographic meanders influence protist community function and structure in the southern Indian Ocean. *Environmental Microbiology*, 25(12), 3161–3179. Available from: <https://doi.org/10.1111/1462-2920.16500>